J. of Basic Sciences, Cheju Nat'l Univ
14(1), 23~28, 2001

기초과학연구 제주대학교
14(1), 23~28, 2001

Eikonal Model Analysis of $^{16}O+^{16}O$ Elastic Scattering at E_{lab} =704 MeV

Yong Joo Kim* and Hye Young Moon†

* *Department of Physics and Research Institute for Basic Sciences, Cheju National University, Jeju 690-756*
and † *Department of Physics, Cheju National University, Jeju 690-756*

The elastic scattering angular distributions of ^{16}O + ^{16}O system at E_{lab} = 704 MeV are analyzed using the first-order eikonal model based on Coulomb trajectories of colliding nuclei. The oscillatory structure observed in the elastic angular distribution could be explained due to the interference between the near- and far-side scattering amplitudes. The features of effective potential and phase shift obtained from the first-order eikonal model are investigated. The strong real and weak imaginary optical potentials are found and they support the presence of nuclear rainbow in the angular distribution of this system.

I. INTRODUCTION

In the early 1970's, the elastic scattering between heavy-ion reaction was born as a field of the nuclear physics in a great expectation. The heavy-ion elastic scattering is generally dominated by the strong absorption, which the implication that the data are only sensitive to the surface of the interaction region and, therefore, the optical potential required to describe the measurements is not uniquely determined. However, the angular distribution for light heavy-ion elastic scattering such as ^{12}C + ^{12}C and ^{16}O + ^{16}O systems has shown the presence of strong refractive effects with a clear signature of a nuclear rainbow phenomena [1,2]. Such a behavior was identified as being a typical refraction effect generated by the nuclear rainbow. The nuclear rainbows seen in the elastic scattering angular distributions of lighter heavy-ion systems unambiguously determine the major features of the optical potential.

Over the past several years, the eikonal approximation [3] has been a useful tool to describe the heavy-ion elastic scattering. A number of studies [4-8] have been made to describe the elastic scattering processes between heavy ions within the framework of the eikonal model. The first- and second-order non-eikonal corrections to the Glauber model have been developed to investigate the possibility of observing a bright interior in the nucleus "viewed" by intermediate energy alpha particle (E_α = 172.5 MeV), as a probe for the ^{58}Ni nucleus [9]. In our previous paper [10], we have presented the first- and second-order corrections to the zeroth-order eikonal phase shifts for heavy-ion elastic scatterings based on Coulomb trajectories of colliding nuclei and it has been applied satisfactorily to the ^{16}O + ^{40}Ca and ^{16}O + ^{90}Zr systems at E_{lab} = 1503 MeV. The elastic scatterings of $^{12}C + ^{12}C$ system at E_{lab} = 240, 360 and 1016 MeV are analyzed using the first-order non-eikonal correction to the eikonal phase shift [11].

In recent, the ^{16}O + ^{16}O elastic cross sections have been measured at 22 MeV/u in a large angular range with high accuracy, and these data showed a nuclear rainbow structure with unambiguous clarity [2]. The elastic scattering data of this system at E_{lab} = 250, 350 and 480 MeV were measured and analyzed within the optical model using the density-dependent folding potential [12]. The elastic scattering angular distributions of this system at E_{lab} = 350 and 480 MeV have been analyzed within the framework of the Coulomb-modified Glauber model by matching the Gaussian density parameters to the modified Fermi ones [13]. In this work, we analyze the elastic scattering angular distributions of the $^{16}O+^{16}O$ system at E_{lab}=704 MeV by using the phase shift analysis within the framework of the first-order eikonal model. The presence of nuclear rainbow is examined. We also investigate some features of the effective optical potential and

phase shift. In section II, we present the theory related with first-order eikonal model. Section III contains the results and discussions. Finally, section IV concludes the paper.

II. THEORY

The general expression of the differential cross section between two identical spinless nuclei is given by the following formula

$$\frac{d\sigma}{d\Omega} = |f(\theta) + f(\pi - \theta)|^2, \qquad (1)$$

where elastic scattering amplitude $f(\theta)$ is given by the equation

$$f(\theta) = f_{\rm R}(\theta) + \frac{1}{ik}\sum_{L=0}^{\infty}(L+\frac{1}{2})\exp(2i\sigma_L) (S_L^{\rm N} - 1)P_L(\cos\theta)\,. \qquad (2)$$

Here $f_{\rm R}(\theta)$ is the usual Rutherford scattering amplitude, k is the wave number and σ_L the Coulomb phase shifts. The nuclear S-matrix elements S_L^N can be expressed by the nuclear phase shifts δ_L

$$S_L^N = \exp(2i\delta_L). \qquad (3)$$

In this work, we use eikonal phase shifts based on the Coulomb trajectories of the colliding nuclei. The Coulomb-modified eikonal phase shift and its first-order correction are given by [10]

$$\delta_L^0(r_c) = -\frac{\mu}{\hbar^2 k}\int_0^\infty U(r)\,dz, \qquad (4)$$

$$\delta_L^1(r_c) = -\frac{\mu^2}{2\hbar^4 k^3}\left(1 + r_c\frac{d}{dr_c}\right)\int_0^\infty U^2(r)\,dz, \qquad (5)$$

where $r = \sqrt{r_c^2 + z^2}$, μ is the reduced mass and the distance of closet approach r_c is given by

$$r_c = \frac{1}{k}\left\{\eta + \left[\eta^2 + (L+\frac{1}{2})^2\right]^{1/2}\right\}, \qquad (6)$$

with the Sommerfeld parameter η.

The zeroth-order term in this expansion is the ordinary Coulomb-modified eikonal phase shift function, while the corrections given by first-order term correspond to non-eikonal effects. The first-order eikonal correction term of the phase shift, $\delta_L^1(r_c)$ in Eqs. (5), can further be expressed as following

$$\delta_L^1(r_c) = -\frac{\mu^2}{\hbar^4 k^3}\int_0^\infty \left[U^2(r) + rU(r)\frac{dU(r)}{dr}\right] dz\,. \qquad (7)$$

The closed expression of the effective phase shift function including up to the first-order correction term may be written as

$$\delta_L(r_c) = -\frac{\mu}{\hbar^2 k}\int_0^\infty U_{\rm eff}(r)\,dz\,, \qquad (8)$$

where $U_{\rm eff}(r)$ is the effective optical potential given by

$$U_{\rm eff}(r) = U\left\{1 + \frac{\mu}{\hbar^2 k^2}\left[U + r\frac{dU}{dr}\right]\right\}. \qquad (9)$$

We can see that the phase shift calculation including non-eikonal corrections up to the first-order is equivalent to a zeroth-order calculation with effective potential $U_{\rm eff}(r)$. By taking $U(r)$ as the optical Woods-Saxon forms given by

$$U(r) = -\frac{V_0}{1+e^{(r-R_v)/a_v}} - i\frac{W_0}{1+e^{(r-R_w)/a_w}}, \qquad (10)$$

with $R_{v,w} = r_{v,w}(A_1^{1/3} + A_2^{1/3})$, we can use the phase shifts, Eqs.(4)-(5) in the general expression for the elastic scattering amplitude, Eqs.(1) and (2).

III. RESULTS AND DISCUSSIONS

As in the preceding section, the Coulomb-modified eikonal model δ_L^0 and δ_L^1 have been used to calculate the elastic differential cross sections for ^{16}O + ^{16}O system at $E_{\rm lab}$= 704 MeV. Table I shows the parameters of the fitted Woods-Saxon potential. The six potential parameters are adjusted so as to minimize the χ^2/N given by

$$\chi^2/N = \frac{1}{N}\sum_{i=1}^{N}\left[\frac{\sigma_{exp}^i - \sigma_{cal}^i}{\Delta\sigma_{exp}^i}\right]^2 \qquad (11)$$

In Eq.(11), σ_{exp}^i (σ_{cal}^i) and $\Delta\sigma_{exp}^i$ are the experimental (calculated) cross sections and uncertainties, respectively, and N is the number of data used in the fitting. The calculated results of the differential cross sections for the elastic scattering of ^{16}O + ^{16}O system at $E_{\rm lab}$= 704 MeV is presented in Fig.1 together with those measured experimentally [14]. In this figure, the dashed curve is the result for zero-order eikonal phase shift, while

TABLE I: Parameters of the fitted Woods-Saxon potential by using the first-order eikonal model analysis for the ^{16}O + ^{16}O elastic scattering at E_{lab}= 704 MeV. 10 % error bars are adopted to obtain χ^2/N value.

V_0 (MeV)	r_v (fm)	a_v (fm)	W_0 (MeV)	r_w (fm)	a_w (fm)	σ_R (mb)	χ^2/N δ^0	χ^2/N $\delta^0+\delta^1$
179	0.844	0.797	42.0	1.099	0.578	1513	9.34	6.54

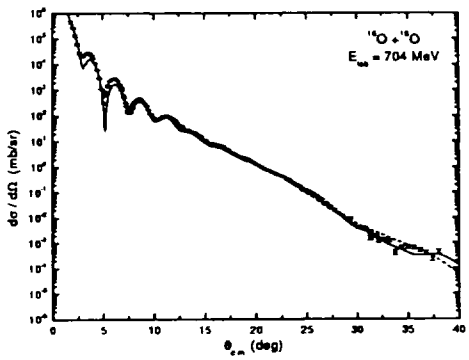

FIG. 1: Elastic scattering angular distributions for ^{16}O + ^{16}O system at E_{lab}= 704 MeV. The solid circles denote the observed data taken from Ref.[14]. The solid and dashed curves are the results for first- and zeroth-order eikonal corrections, respectively.

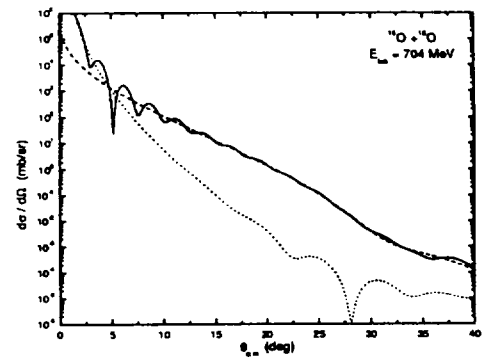

FIG. 2: Differential cross section (solid curves), near-side contribution (dotted curves), and far-side contribution (dashed curves) obtained by the Fuller's formalism [15] using the first-order eikonal model for ^{16}O + ^{16}O system at E_{lab}= 704 MeV.

the solid curve is the first-order eikonal phase shift. As seen in this figure, the differences between the dotted and solid curve are substantial when compared with the experimental data. The present results including first-order eikonal correction can reproduce satisfactorily the observed data over the whole angular range. Also, the reasonable χ^2/N values is obtained in the ^{16}O + ^{16}O system at E_{lab}= 704 MeV as listed in table I.

In order to understand the nature of angular distributions for ^{16}O + ^{16}O system at E_{lab}= 704 MeV, the near- and far-side decompositions of scattering amplitudes are also performed with the first-order correction to the eikonal phase shifts by following Fuller's formalism [15]. The contribution of the near- and far-side components to the elastic scattering cross sections are shown in Fig. 2 along with the differential cross section. The differential cross section is not just a sum of the near- and far-side cross sections but contains the interference between the near- and far-side amplitudes as shown in Fig. 2. The refractive oscillation observed on the elastic scattering angular distribution of ^{16}O + ^{16}O system at E_{lab}=704 MeV is due to the interference between the near- and far-side components. The magnitude of the near- and far-side contributions is equal, crossing point, at $\theta = 4.8°$ for this reaction. This figure shows the near-side dominance at angles less than this value due to the long-range repulsive Coulomb interaction. However, the far-side scattering has become dominant at the regions greater than the crossing angle due to the short-range attractive nuclear interaction.

The transmission function $T_L = 1 - |S_L|^2$ is plotted versus the orbital angular momentum in Fig.3, along with the deflection function. The transmission function can be explained using the imaginary part of the effective optical potential. As shown Fig. 3(a), the lower partial waves are totally absorbed and the T_L is decreased very rapidly in a narrow localized angular momenta zone. The presence of nuclear rainbow can be proved by investigating the deflection function given by $\theta_L = 2\frac{d}{dL}(\sigma_L + \text{Re } \delta_L)$. In a rainbow situation, the strong nuclear force attracts the projectiles towards the scattering center and deflects them to negative angle, which correspond to the region of the rainbow maximum.

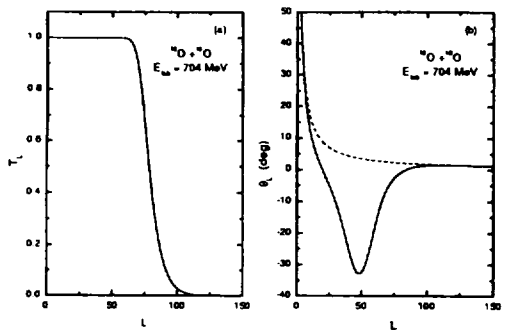

FIG. 3: (a) Transmission function T_L and (b) deflection function for $^{16}O + ^{16}O$ system at E_{lab}= 704 MeV plotted versus the orbital angular momentum L in the first-order eikonal model. The dashed curve represents the deflection function for the Coulomb phase shift.

In Fig. 3(b), we can find the nuclear rainbow angle value $\theta_{nr} = -33.0°$, which evidently prove a presence of the nuclear rainbow with unambiguous clarity in this system.

In order to illustrate the difference between the effective and nominal potentials, we plot the real and imaginary parts of this potential in Fig. 4. Figure 4(a) and 4(b) present the real and imaginary part of optical potential, respectively. The solid curves are the first-order effective potentials $U_{eff}(r)$ given by Eq.(9), while the dashed curves are the results of nominal potential $U(r)$. As shown in this figure, there is a dramatic difference between the two potentials, especially for the imaginary part. We can see in Eq.(9) that the effective imaginary potential with the first-order eikonal correction depends on the product of the real and imaginary potentials and their derivatives. Thus the effective imaginary potentials rapidly increase until they reach maximum value in the central region of the nucleus, and then they reach minimum in the surface region. A drastic increase of the imaginary potential for small values of r corresponding to increased transmission is mainly due to the correction term in Eq.(9). In the traditional optical model, it is assumed that the imaginary part of the potential is responsible for the absorption process in the nuclear reaction and its shape should not be affected by the real part. Nevertheless, in the present eikonal model with the first-order correction, we can find that the drastic increase on the absorptive potential in the small r region are due to the larger real potential compared with imaginary one. Figure 4(c) shows

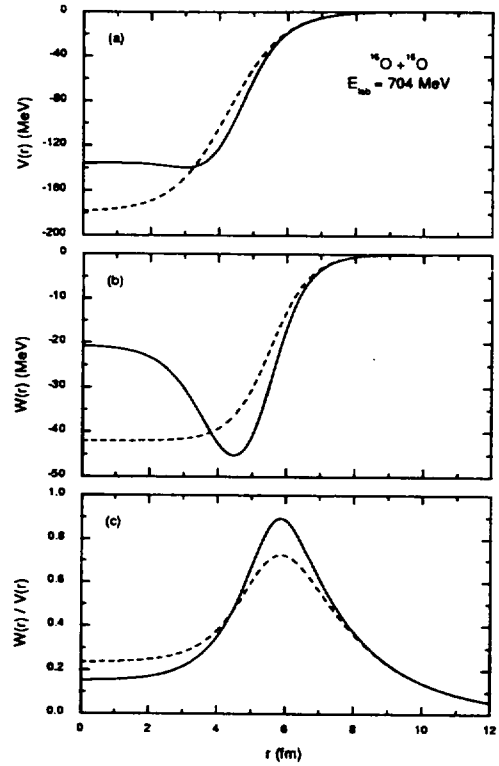

FIG. 4: (a) Real , (b) imaginary and (c) the ratio of imaginary to real part, of the optical potential for the $^{16}O + ^{16}O$ system at E_{lab}= 704 MeV. The solid and dashed curves are the results for first- and zeroth-order eikonal corrections, respectively.

the "reduced imaginary potential", the ratio of imaginary to real optical potential. In this figure, we find some remarkable feature. In the small r region, the effective imaginary potential of the first-order eikonal model is small compared with the effective real potential. Such a small ratio makes it possible to interpenerate each other between the projectile and target nuclei. As a result the projectile ion can penetrate the nuclear surface barrier of the target, and the cross section becomes sensitive to the value of the real potential in the central region. In the large r region, the real and imaginary parts of the effective potential have exponential tail approaching zero. We can also see that the first-order eikonal model has a larger peak value of the reduced imaginary potential compared to one of zeroth-order eikonal model.

Such increase of the effective potential in the small region is also reflected in the phase shift function. Figure 5 show angular mo-

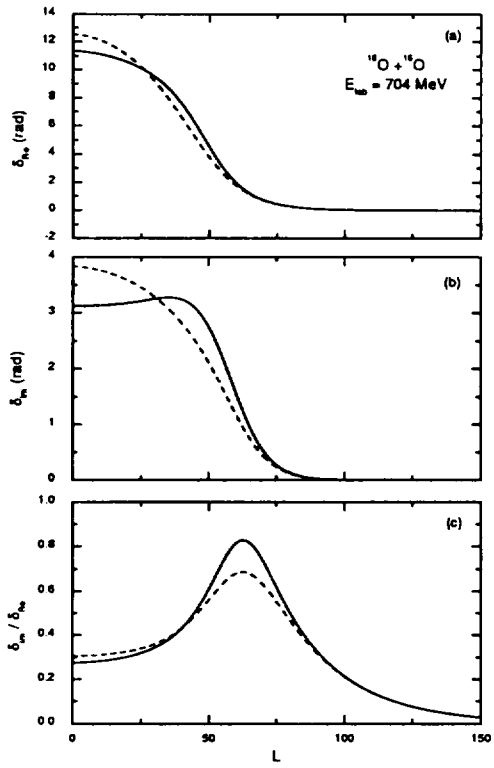

FIG. 5: (a) Real , (b) imaginary and (c) the ratio of imaginary to real part, of the eikonal phase shift for the ^{16}O + ^{16}O system at E_{lab}= 704 MeV. The solid and dashed curves are the results for first- and zeroth-order eikonal corrections, respectively.

mentum dependence of the real and imaginary parts of the eikonal phase shifts calculated with (solid curves) and without (dashed curves) first-order eikonal correction, respectively. The real phase shift vanishes nearly quadratically as the L increases. The real phase shift of the first-order eikonal corrections is less values than the result of zeroth-order eikonal phase shift at $L < 26$ and, however, is greater ones than one of zeroth-order case at $L > 26$. On the other hand, we can find the dramatic variations of the imaginary phase shifts for this system, as expected. The strong absorption in the nuclear surface plays a dominant role to the scattering amplitude and thus to the characteristic diffraction pattern of the angular distribution. The large angle behavior is sensitive to the details of the real optical potential over a wide radial region from the nuclear surface towards the interior. As a result the projectile ion can penetrate the nuclear surface barrier of the target, and the cross section becomes sensitive to the value of the potential in the central region. Figure 5(c) display the "reduced imaginary phase shift", a ratio of imaginary to real part of phase shifts. Comparing Fig. 5(c) with Fig. 4(c), we can find that two figures show very similar structures. Also, the maximum value of phase shift ratio is increase when first-order eikonal correction is included.

IV. CONCLUSIONS

In this work, we have analyzed the elastic scattering of ^{16}O+ ^{16}O system at E_{lab}=704 MeV by using the first-order eikonal model based on the Coulomb trajectories of colliding nuclei. We have found that the results of the present first-order eikonal model are in reasonable agreement with the observed data. Through near- and far-side decompositions of the cross section, we have shown that the refractive oscillation of this system is due to the interference between the near- and far-side amplitude. The presence of a nuclear rainbow is also evidenced by the classical deflection function. The absorption in the ^{16}O + ^{16}O system at E_{lab} = 704 MeV is weak enough to allow refracted projectiles to populate the elastic channel and typical nuclear rainbow effects could be observed in the angular distribution.

We have found that the effect of first-order eikonal correction on the imaginary potential is important when the absorptive potential is weak and the real potential is strong. The strong real potential give a drastic effect on the effective imaginary potential for ^{16}O + ^{16}O system at E_{lab}= 704 MeV. The ratio of imaginary to real part of effective potential is found to be small in the central region. Such a small ratio value makes it possible to interpenetrate each other between the projectile and target nuclei.

We can also see in the imaginary phase shift calculated with the real potential that an absorption of partial waves for large angular momentum increases, whereas the absorption decreases for small angular momentum, compared to the result without the real potential. The reduced imaginary phase shift show similar structure with the reduced imaginary potential, indicating that the reduced imaginary phase shift is very sensitive to the reduced imaginary potential. We can also see that the first-order eikonal model has a larger peak value of the reduced imaginary

phase shift compared to one of the zeroth-order eikonal model.

REFERENCES

[1] M. E. Brandan, Phys. Rev. Lett. **60**, 784 (1988).

[2] E. Stiliaris, H. G. Bohlen, P. Fröbrich, B. Gebauer, D. Kolbert, W. von Oertzen, M. Wilpert and Th. Wilpert, Phys. Lett. **223**, 291 (1989).

[3] D. Waxman, C. Wilkin, J. -F. Fermond and R. J. Lombard, Phys. Rev. C **24**, 578 (1981).

[4] T. W. Donnelly, J. Dubach and J. D. Walecka, Nucl. Phys. Nucl. Phys. **A232**, 355 (1974).

[5] J. Knoll and R. Schaeffer, Ann. Phys. (N.Y.) **97**, 307 (1976).

[6] R. da Silveira and Ch. Leclercq-Willain, J. Phys. G **13**, 149 (1987).

[7] G. Fäldt, A. Ingemarsson and J. Mahalanabis, Phys. Rev. C **46**, 1974 (1992).

[8] C. E. Aguiar, F. Zardi and A. Vitturi, Phys. Rev. **C56**, 1511 (1997).

[9] S. M. Eliseev and K. M. Hanna, Phys. Rev. **C56**, 554 (1997).

[10] M. H. Cha and Y. J. Kim, Phys. Rev. **C51**, 212 (1995).

[11] Y. J. Kim, M. H. Cha, Int. J. Mod. Phys. **E9**, 67 (2000).

[12] D. T. Khoa, W.von Oertzen, H. G. Bohlen, G. Bartnitzky, H. Clement, Y. Sugiyama, B. Gebauer, A. N. Ostrowski, Th. Wilpert and C. Langner, Phys. Rev. Lett. **74**, 34 (1995).

[13] M. H. Cha and Y. J. Kim, Sae Mulli, **40**, 183 (2000).

[14] D. T. Khoa (Private Communication).

[15] R. C. Fuller, Phys. Rev. **C12**, 1561 (1975).